Published by :
http://www.ijert.org

International Journal of Engineering Research & Technology (IJERT)
ISSN: 2278-0181
Vol. 14 Issue 11, November 2025

3D radiative Oldroyd-B fluid flow towards Convectively Heated Surface with Irregular Heat Source and Activation Energy

Y. Veeranna
Department of Studies and Research in Mathematics, Government Science College (Autonomous), Bengaluru-560 001, Karnataka, India.

Abstract: Three dimensional MHD (magnetohydrodynamic)flow of radiative Oldroyd-B fluid over a convectively heated stretched sheet is investigated. The influence of irregular heat source, suction and activation energy are also studied. The Appropriate transformations are used reduce a system of nonlinear partial differential equations into a system of ordinary differential equations. The numerical solution are reported by RKF method. The diverse liquid flow characteristics are examined for various involved parameters through graphs and tables. It is exposed that, the Deborah numbers (β_1, β_2) have quite opposite behaviour on flow field. The liquid temperature is increase when increasing in irregular heat sources. The effect of activation energy is favourable to concertation profile.

Keywords: Oldroyd-B fluid; irregular heat sources; activation energy; thermal radiation,

Introduction

Fluid streams are existing universally in nature and vital to plants, animals and people living on earth. In current years, the study of non-Newtonian fluids has gained a great attention of engineers and scientists due to its significant applications in industries and technology. These applications can be found mainly in chemical and nuclear industries, food and pharmaceutical industries, material processing, geophysics and biomedical engineering. As a consequence of different physical structures of non-Newtonian fluids, there is not a single constitutive model which can predict all its salient features. Generally, there are three non-Newtonian fluid models, namely empirical models, differential models and integral models. In present work, we have studied the second model and consider its subclass known as Oldroyd-B fluid. The major properties of the Oldroyd-B model was proposed to determine the relaxation time and retardation time, which cannot be explored by the Maxwell fluid model. On the other hand, it has a measurable retardation time and can relate the viscoelastic manner of dilute polymeric solutions under general flow conditions. The idea of the boundary layer flow of the Oldroyd-

International Journal of Engineering Research & Technology (IJERT)
ISSN: 2278-0181
Vol. 14 Issue 11, November 2025

B liquid induced by the linear stretching of a surface was first initiated by Sajid et al. [1]. They presented that the numerical solution of boundary layer flow of an Oldroyd-B fluid in the region of stagnation point past a stretching sheet using finite difference method. Many investigators have extended the work of Sajid et al. [1]. Shehzad et al. [2] deliberated the three-dimensional flow of the Oldroyd-B fluid with the effects of temperature-dependent thermal conductivity, and considered that the fluid flow generating due to the bidirectional stretching of the surface. The effects of the temperature stratification in a steady-state Oldroyd-B liquid flow at the stagnation point with mixed convection was investigated by Hayat et al. [3]. They reported the analytic solutions for velocity and temperature using homotopic analysis method. Motsa et al. [4] addressed the temperature dependent three-dimensional flow of Oldroyd-B fluid with heat source/sink effects by spectral relaxation technique. Hayat et al. [5] have discussed convergence of series solutions for the steady flow of an Oldroyd-B fluid induced by an exponentially stretched surface using homotopy analysis technique. Mahanthesh et al. [6] addressed the effect of non-linear convection in a laminar three-dimensional Oldroyd-B fluid flow and the heat transfer phenomenon is explored by considering the non-linear thermal radiation and heat generation/absorption. Some recent investigations on Oldroyd-B fluid flows can be found in Refs. [7]-[10].

The influence of thermal radiation significantly affects the rate of heat transfer and the temperature distributions in the boundary layer flow of participating fluid. So, the radiation effect have many industrial and engineering applications, such as space technology, nuclear power plants, in aircraft and also in gas turbines and controlling heat transfer processes in engineering fields. There are many research have made to predict the effect of thermal radiation with different aspects (see Makinde [11] - Hayat et al. [17]). However, all these works deals with influence of linear thermal radiation, but in recent time; the idea of nonlinear radiation has attracted many researchers. For the reason that, linear radiation is valid only for small temperature differences within the fluid, it is not sufficient in scientific and engineering applications in which the working fluids having the small temperature differences. In fact, the researchers have interested to consider nonlinear thermal radiation influence by assuming large temperature difference. In view of this, Pantokratoras and Fang [18] were first to investigated the effect of nonlinear radiation on the Sakiadis flow. They have analyzed great temperature differences within the fluid. They found that, nonlinear radiation effect significantly affects the formation thermal boundary layer when comparison with linear radiation. Mushtaq et al. [19] reported the numerical solutions for nonlinear

International Journal of Engineering Research & Technology (IJERT)
ISSN: 2278-0181
Vol. 14 Issue 11, November 2025

radiative flow and heat transfer of nanofluid due to solar energy. Cortell [20] investigated the fluid flow and heat transfer over a stretching sheet with considered the Rosseland approximations to non-linearize the thermal radiation term in energy equation.Shehzad et al. [21] have scrutinised the nonlinear thermal radiation effect on non-Newtonian Jeffery fluid flow with suspended nanoparticles. Hayat et al [22] presented the analytical solutions for magnetohydrodynamic flow and radiative heat transfer of nanofluid under velocity slip boundary by HAM method. Sampath et al. [23] presented the numerical solutions for nonlinear radiative rotating flow of Ferrofluid with Joule heating and convective condition using RKF technique. Furthermore, the nonlinear thermal radiation effect on different problems of the fluid flows have been treated by various investigators(Mahanthesh et al. [24],Farooq et al. [25]. Laxmi and Shankar [26]. Jayachandra et al. [27]).

In this work, reported the similarity solutions for nonlinear radiative heat transfer in three-dimensional flow of an Oldroyd-B fluid induced by the bidirectional stretching surface. We also consider the irregular heat source, suction and activation energy effects in the heat transfer expressions. The convective boundary condition is employed at the boundary surface. With the help of similarity transformations, the governing PDE system is reduced to nonlinear ODE system then the mathematical model is undertaken through the 4-5th order RK-Fehlberg techniques via the shooting algorithm. The physical consequence of scheming parameters on the velocity, temperature and concentration fields are inspected and deliberated graphically.

Mathematical formulation

We consider three dimensional radiative flow of an Oldroyd-B fluid over a stretching sheet. The sheet coincides with the plane at z = zero and it establish in to the space z> zero as shown in Fig. 1. By keeping origin fixed and the sheet is elaborate in to bidirectional (x and y) with velocity$u_w = ax$ and $v_w = by$. The sheet is heated by a hot fluid with temperature T_f which is related with the heat transfer coefficients h_f and T_∞ and C_∞ as temperature and concentration far away from the surface.

Published by :
http://www.ijert.org

International Journal of Engineering Research & Technology (IJERT)
ISSN: 2278-0181
Vol. 14 Issue 11, November 2025

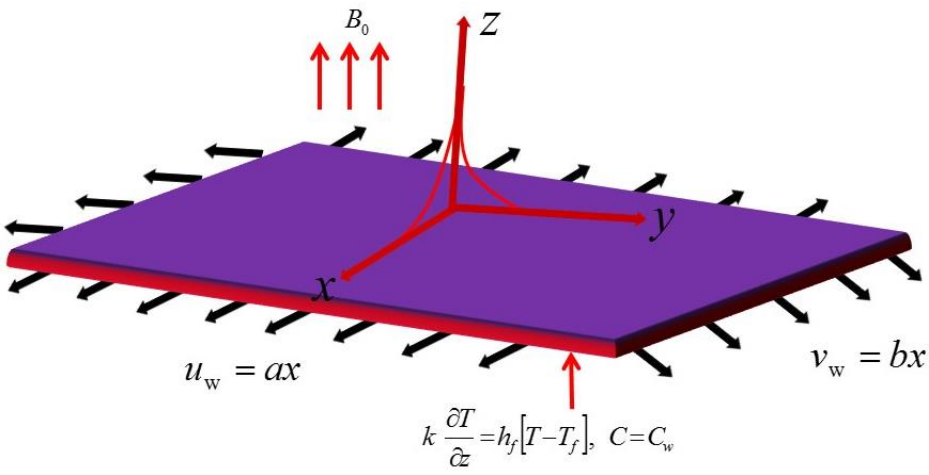

Figures 1: Geometry of the problem

The simplified three dimensional boundary layer equations of continuity, momentum, heat and variation of concentration with subjected to the boundary layer assumption are;

$$\frac{\partial u}{\partial x} + \frac{\partial v}{\partial y} + \frac{\partial w}{\partial z} = 0, \tag{1}$$

$$u\frac{\partial u}{\partial x} + v\frac{\partial u}{\partial y} + w\frac{\partial u}{\partial z}$$

$$+\lambda_1\left(u^2\frac{\partial^2 u}{\partial x^2} + v^2\frac{\partial^2 u}{\partial y^2} + w^2\frac{\partial^2 u}{\partial z^2} + 2uv\frac{\partial^2 u}{\partial x\partial y} + 2vw\frac{\partial^2 u}{\partial y\partial z} + 2uw\frac{\partial^2 u}{\partial x\partial z}\right)$$

$$= \nu\left(\frac{\partial^2 u}{\partial z^2} + \lambda_2\left(u\frac{\partial^3 u}{\partial x\partial z^2} + v\frac{\partial^3 u}{\partial y\partial z^2} + w\frac{\partial^3 u}{\partial z^3} - \frac{\partial u}{\partial x}\frac{\partial^2 u}{\partial z^2} - \frac{\partial u}{\partial y}\frac{\partial^2 v}{\partial z^2} - \frac{\partial u}{\partial z}\frac{\partial^2 w}{\partial z^2}\right)\right) - \sigma\frac{B_0^2}{\rho}u \tag{2}$$

$$u\frac{\partial v}{\partial x} + v\frac{\partial v}{\partial y} + w\frac{\partial v}{\partial z}$$

$$+\lambda_1\left(u^2\frac{\partial^2 v}{\partial x^2} + v^2\frac{\partial^2 v}{\partial y^2} + w^2\frac{\partial^2 v}{\partial z^2} + 2uv\frac{\partial^2 v}{\partial x\partial y} + 2vw\frac{\partial^2 v}{\partial y\partial z} + 2uw\frac{\partial^2 v}{\partial x\partial z}\right)$$

$$= \nu\left(\frac{\partial^2 v}{\partial z^2} + \lambda_2\left(u\frac{\partial^3 v}{\partial x\partial z^2} + v\frac{\partial^3 v}{\partial y\partial z^2} + w\frac{\partial^3 v}{\partial z^3} - \frac{\partial v}{\partial x}\frac{\partial^2 v}{\partial z^2} - \frac{\partial v}{\partial y}\frac{\partial^2 v}{\partial z^2} - \frac{\partial v}{\partial z}\frac{\partial^2 w}{\partial z^2}\right)\right) - \sigma\frac{B_0^2}{\rho}v \tag{3}$$

$$u\frac{\partial T}{\partial x} + v\frac{\partial T}{\partial y} + w\frac{\partial T}{\partial z} = \alpha_m\frac{\partial^2 T}{\partial z^2} + \frac{Q_T}{\rho c_p}(T - T_\infty) - \frac{1}{\rho c_p}\frac{\partial q_r}{\partial z} + \frac{Q_E}{\rho c_p}(T_f - T_\infty)e^{-ny\sqrt{\frac{a}{\nu}}} \tag{4}$$

$$u\frac{\partial C}{\partial x} + v\frac{\partial C}{\partial y} + w\frac{\partial C}{\partial z} = D_B\frac{\partial^2 C}{\partial z^2} - k_r{}^2(C - C_\infty)\left(\frac{T}{T_\infty}\right)^n exp\left(\frac{-E_a}{KT}\right) \tag{5}$$

Where u, v and w are the velocities along the $x, y,$ and z -directions, T - temperature, λ_1 andλ_2 are the relaxation and retardation time, ν -kinematic viscosity , $\beta_0$and$\beta_1$are the volumetric thermal expansion coefficients, $\alpha_m = k/(\rho C_p)$ is fluid thermal diffusivity of the

International Journal of Engineering Research & Technology (IJERT)
ISSN: 2278-0181
Vol. 14 Issue 11, November 2025

fluid , k -thermal conductivity , ρ -density of the fluid , C_p -specific heat of the fluid , Q_0-heat generation / absorption coefficient and q_r -radiative heat flux.

The thermal radiation heat flux expression through the Rosseland approximation is

$$q_r = -\frac{16\sigma^*}{3k_1}T^3\frac{\partial T}{\partial z} \tag{6}$$

Where k_1 -mean absorption coefficient, , and σ^* -Stefan – Boltzmann constant

From equation (4), we obtained

$$u\frac{\partial T}{\partial x} + v\frac{\partial T}{\partial y} + w\frac{\partial T}{\partial z}$$

$$= \frac{\partial}{\partial z}\left(\left(\alpha_m + \frac{16\sigma^*}{3\rho k_1 C_p}T^3\right)\frac{\partial T}{\partial z}\right) + \frac{Q_T}{\rho c_p}(T - T_\infty) + \frac{Q_E}{\rho c_p}(T_f - T_\infty)e^{-ny\sqrt{\frac{a}{v}}} \tag{7}$$

For the present problem corresponding boundary conditions are

$$u = u_w, \quad v = v_w, \quad w = 0, \quad k\frac{\partial T}{\partial z} = h_f(T - T_f), \quad C = C_w \quad \text{at} \quad z = 0$$

$$u \to 0, \quad v \to 0, \quad \frac{\partial u}{\partial z} \to 0, \quad \frac{\partial v}{\partial z} \to 0, \quad T \to T_\infty, \quad C \to C_\infty \text{ as } \quad z \to \infty \tag{8}$$

The above partial differential equations transformed into the corresponding nonlinear ordinary differential equations by setting correct similarity variables as follows

$$u = axf'(\eta), \quad v = ayg'(\eta), \quad w = -\sqrt{va}(f(\eta) + g(\eta)),$$

$$T = T_\infty + \theta(\eta)(T_f - T_\infty), \quad \phi(\eta) = \frac{C - C_\infty}{C_w - C_\infty}, \quad \eta = \sqrt{\frac{a}{v}}z. \tag{9}$$

Here the prime denoted by derivative with respective to η . in the above equations

We get the following set of non-linear ordinary differential equations.

$$f''' + (f+g)f'' - f'^2 + \beta_1(2(f+g)f'f'' - (f+g)^2 f''')$$

$$+\beta_2((f''+g'')f'' - (f+g)f'''') - Mf' = 0 \tag{10}$$

$$g''' + (f+g)g'' - g'^2 + \beta_1(2(f+g)g'g'' - (f+g)^2 g''')$$

$$+\beta_2((f''+g'')g'' - (f+g)g'''') - Mg' = 0 \tag{11}$$

International Journal of Engineering Research & Technology (IJERT)
ISSN: 2278-0181
Vol. 14 Issue 11, November 2025

$$\frac{1}{p_r}(\,(\,1+R(1+(\theta_w-1)\theta)^3)\theta')'+(\,f+g)\theta'+Q_t\theta+Q_e\exp(-n\eta)=0 \qquad (12)$$

$$\phi''+Sc(f+g)\phi'-\sigma Sc\,\phi(1+\sigma\theta)^n\exp\left(-\frac{E}{1+\delta\theta}\right)=0 \qquad (13)$$

Where $Q_t=\frac{Q_T}{\rho c_p a}\rightarrow$ temperature Heat source,

$Q_e=\frac{Q_E}{\rho c_p a}\rightarrow$ Exponential space dependent Heat source. $\eta=z\sqrt{\frac{a}{\nu}}$

The boundary conditions for the present problem are

$$f'(\eta)=1\,,\ g'(\eta)=C_1,\ f'(\eta)=0\ \ g(\eta)=0\ \phi(\eta)=1$$
$$g(\eta)=0\,,\theta'=Bi(\theta(\eta)-1)at\eta=0 \qquad (14)$$

$$f'\rightarrow 0\,,f''\rightarrow 0\,,g'\rightarrow 0\,,g''\rightarrow 0\,,\theta\rightarrow 0\ as\eta\rightarrow\infty\,, \qquad (15)$$

Where the dimensionless parameters are

$$\beta_1=\lambda_1 a,\ \ \beta_2=\lambda_2 a\ \ C_1=\frac{b}{a},\qquad \lambda=\frac{Gr_x}{Re_x{}^2},\quad Re_x=\frac{xu_w}{\nu}\,Gr_x=\frac{g_v\beta_0(T_f-T_\infty)x^3}{v^2},$$
$$R=\frac{16\,\sigma T_\infty{}^3}{3k_1k},\qquad \theta_w=\frac{T_f}{T_\infty}\qquad S=\frac{Q_t}{a\rho C_p},\quad P_r=\frac{\mu C_p}{k},\quad B_i=\frac{h_f}{k\sqrt{\frac{a}{\nu}}}$$

Here we observe from the above equations $\lambda_1$and $\lambda_2$are the relaxation time and retardation time. v-kinamatic viscosity,ρ-density of the fluid,B_0 – strength of magnetic field , $M=\frac{\sigma B_0{}^2}{\rho a}$- Magnetic parameter,$c_p$ -specific heat Tf -fluid temperature, n - velocity power index parameter, $k_r{}^2$ - reaction rate, $E=\frac{E_a}{kT_\infty}$ - non-dimensional energy , E_a - activation energy, $\theta_w=\frac{T_f}{T_\infty}$ - Temperature ratio parameter , $S_C=\frac{\nu}{D_B}$ -Schmidt number , $Q_t=\frac{Q_T}{\rho c_p a}$ - temperature heat source,$Q_e=\frac{Q_E}{\rho c_p a}$ exponential space dependent heat source ,$\beta_1=\lambda_1 a$and $\beta_2=\lambda_2 a$ are the Deborah numbers, $c=\frac{b}{a}$ -stretching ratio parameter, , $Re_x=\frac{xu_w}{\nu}$ Reynolds number,$R=\frac{16\,\sigma T_\infty{}^3}{3k_1k}$ is the thermal radiation parameter, $\theta_w=\frac{T_f}{T_\infty}$ temperature ratio parameter, $S=\frac{Q_0}{a\rho C_p}$ is the heat source / sink parameter, $P_r=\frac{\mu C_p}{k}$ prandtl number and $B_i=\frac{h_f}{k\sqrt{\frac{a}{\nu}}}$ is the Biot number.

In the engineering applications the physical quantity of the boundary value problems, the skin frication, local Nusselt number (Nu) and Sherwood number $(Shx)$are denoted by

International Journal of Engineering Research & Technology (IJERT)
ISSN: 2278-0181
Vol. 14 Issue 11, November 2025

$$N_u = \frac{u_w q_w}{ak(T_f - T_\infty)}, \quad \text{Nusselt number} \tag{15}$$

Where q_w is the surface heat flux with the similarity variables, we obtain

$$\frac{N_u}{\sqrt{Re_x}} = -\left(1 + R\theta_w{}^3\right)\theta'(0) \tag{16}$$

$$Sh_x = \frac{u_w J_w}{aD_B(C_w - C_\infty)}, \tag{17}$$

Where J_w is the concentration flux. with the similarity variables, we obtain

$$\frac{Sh_x}{\sqrt{Re_x}} = -\phi'(0) \tag{18}$$

Results and Discussion

A set of nonlinear ordinary differential equations (2.10)-(2.13) with boundary conditions are regenerate to a set of linear ordinary differential equations by acceptable substitutions. Then resultant equations are treated as numerically using RKF technique. During this theme, it's most important to set the suitable finite values of η_{max}. In accordance with standard practice in the boundary layer theory the asymptotic boundary conditions at η_{max} arereplaced byη_8. In our numerical computations, the step size is select as $\Delta\eta = 0.001$ and therefore the convergence criteria were set to10^{-6}. In this section devoted to analyze the effect of the assorted physical parameters involved in the fluid flow problem, such as magnetic parameter(M), Deborah numbers (β_1, β_2), stretching ratio parameter(C_1), Biot number (B_i), temperature and exponentially space dependent heat source parameters (Q_t, Q_e), radiation parameter(R), temperature ratio parameter(θ_w), temperature difference parameter (δ), activation energy parameter (E), Schmidt number $(Sc)$and dimensionless reaction rate parameter (σ).

The variation of velocity profiles $f'(\eta)$and $g'(\eta)$for M is displayed in Fig. 2.The strong magnetic field produces a Lorentz force (resistive force). The resistive force opposes to liquid flow at the surface, as a result the velocity profiles with related boundary layer thickness decreases. Impact of β_1 on velocity profiles is illustrated in Fig. 3. It is observed

International Journal of Engineering Research & Technology (IJERT)
ISSN: 2278-0181
Vol. 14 Issue 11, November 2025

that, the $f'(\eta)$and $g'(\eta)$ are reduces for higher β_1. This mechanism due to the fact that the Deborah number $\beta_1$depends on relaxation time. The increase in the relaxation time leads to diminish the liquid flow and their boundary layer thickness. Fig. 4indicated that the influence of the β_2 on $f'(\eta)$and $g'(\eta)$. It is confirm that augment the liquid velocity for higher β_2.Physically the Deborah number$\beta_2$generates the retardation time. The high retardation time diminishes the viscous property of working liquid which causes increase in $f'(\eta)$and $g'(\eta)$.

The effect of C_1(stretching ratio parameter) on the $f'(\eta)$and $g'(\eta)$is displayed in Fig. 5. It is remark that, decay the velocity field$f'(\eta)$while the velocity field$g'(\eta)$ is increases. The reason behind that an increase in $C_1$is leads to the movement of the lateral surface in the y-direction that corresponds to increase the momentum boundary layer thickness. Impact of Bi on $\theta(\eta)$ and $\phi(\eta)$ is plotted in Fig. 6. It is clearly shows that, the higher values of Bi is enhance the $\theta(\eta)$ but quit opposite trend has been observed in $\phi(\eta)$.Behaviour of Q_s and Q_t on temperature field$\theta(\eta)$ and concentration field$\phi(\eta)$ are depicted in figure 7 and 8 respectively. It is noted that, the liquid concentration is reduces while the liquid temperature is augmented via higher values of Q_s and Q_t. By enhancing the values of Q_s and Q_t provides extra heat from surface towards working fluid (Oldroyd-B fluid), in fact the fluid temperature and their related thermal boundary layer thickness is increase.

Figures 9-10 indicate the impact of R and θ_w on $\theta(\eta)$ and $\phi(\eta)$. It clearly shows that, the higher values of R and θ_w as increase the temperature distribution but opposite behaviour is occurs in concentration profile. Heat creates in liquid flow through radiation mechanism and the surface become warm for higher$\theta_w (= T_f/T_\infty)$, as a result the thermal boundary layer become thicker. The variation of temperature difference parameter δ on $\phi(\eta)$ is plotted in Fig. 11. It is noted that the higher values of δ is diminishes $\phi(\eta)$.The reason behind that, the higher $\delta = ((T_f - T_\infty)/T_\infty)$increases the wall temperature and decreases the ambient

International Journal of Engineering Research & Technology (IJERT)
ISSN: 2278-0181
Vol. 14 Issue 11, November 2025

temperature. However, the liquid concentration decrease. Fig. 12 represent the concentration profiles for various values of E. It is reported that the impact of activation energy Eleads to increases in $\phi(\eta)$. Due to higher values of Eleads to lesser reaction rate constant and consequently slow down the chemical reaction, as a result increases in $\phi(\eta)$.The impact of Sc and σ on $\phi(\eta)$ are illustrated in Fig. 13 and 14 respectively. We can see that diminishing in concentration boundary layer when $Sc$and σ are increased. Physically, an higher Sc generates the lower solute diffusivity then reduction accurse in $\phi(\eta)$.

Numerical solutions of $f''(0), g''(0), Nu/Re_x^{0.5}$ and $Sh/Re_x^{0.5}$ for different parametric values are reported in table 1. It is clearly shows that, the friction force is more effective for larger M but quit opposite behaviour is seen in $Sh/Re_x^{0.5}$. The rate of heat transfer $Nu/Re_x^{0.5}$ is high for R, θ_w, Bi and Pr but conflicting for M, Q_s, Q_t.The mass transfer rate $Sh/Re_x^{0.5}$ is high for $R, \theta_w, Bi, Q_s, Q_t, M$ and higher values of E, Pr have less mass transfer rate. Table 2 present the numerical data of $f''(0), g''(0), Nu/Re_x^{0.5}$ and $Sh/Re_x^{0.5}$ with varying $Sc, \beta_1, \beta_2, C_1, \delta, n$ and σ.It is reported that no difference is found in drag force $(f''(0), g''(0))$ for Sc, δ, n and σ. For exact opposite behaviour is occurs in $f''(0), g''(0), Nu/Re_x^{0.5}$ and $Sh/Re_x^{0.5}$with varying $\beta_1$and β_2.The $Nu/Re_x^{0.5}$ is increase with higher n and C_1. The Sharwood number $Sh/Re_x^{0.5}$ is enhances for σ, n, δ and Sc but decrease forC_1.

Concluding remarks

3D nonlinear radiative Oldroyd-B fluid flow over an elongated sheet with influence of irregular heat source and activation energy is scrutinized in this paper. The effects of magnetic field, suction and convective condition are also elaborated. The following observations are found;

International Journal of Engineering Research & Technology (IJERT)
ISSN: 2278-0181
Vol. 14 Issue 11, November 2025

- Higher activation energy leads to increase in concertation profile.
- The momentum boundary layer become thinner for high magnetic field strength.
- The impact of β_1 and β_2 are quite opposite behaviour on liquid field characteristics.
- Heat and mass transfer rate is high for R, θ_w and Bi.
- Choose lesser values of thermal radiation to liquid cooling process.
- Increase the liquid temperature for irregular heat sources.

Table 1: Numerical results of $f''(0), g''(0), Nu/Re_x^{0.5}$ and $Sh/Re_x^{0.5}$ for different values of $Bi, E, M, Pr, Q_e, Q_t, R$ and θ_w.

Bi	E	M	Pr	Q_e	Q_t	R	θ_w	$f''(0)$	$g''(0)$	$Nu/Re_x^{0.5}$	$Sh/Re_x^{0.5}$
0.4	2	0.5	1.2	0.1	0.1	0.4	2	-1.20971	-0.66238	0.651255	1.101407
0.4								-1.20971	-0.66238	0.651255	1.101407
0.6								-1.20971	-0.66238	0.716853	1.161491
0.8								-1.20971	-0.66238	0.746018	1.197950
0.4	0							-1.20971	-0.66238	0.651255	1.973478
	2							-1.20971	-0.66238	0.651255	1.101407
	4							-1.20971	-0.66238	0.651255	0.672215
	2	0						-1.04730	-0.55430	0.706060	1.084009
		0.5						-1.20971	-0.66238	0.651255	1.101407
		0.8						-1.29846	-0.72026	0.619114	1.112353
		0.5	0.7					-1.20971	-0.66238	0.447421	1.194781
			1.2					-1.20971	-0.66238	0.651255	1.101407
			1.5					-1.20971	-0.66238	0.736385	1.060731
			1.2	0				-1.20971	-0.66238	0.803187	1.035922
				0.1				-1.20971	-0.66238	0.651255	1.101407
				0.2				-1.20971	-0.66238	0.512402	1.159935
					0			-1.20971	-0.66238	0.759943	1.054070

International Journal of Engineering Research & Technology (IJERT)
ISSN: 2278-0181
Vol. 14 Issue 11, November 2025

					0.1			-1.20971	-0.66238	0.651255	1.101407
					0.2			-1.20971	-0.66238	0.465141	1.181487
						0.4		-1.20971	-0.66238	0.651255	1.101407
						0.6		-1.20971	-0.66238	0.742923	1.153528
						0.8		-1.20971	-0.66238	0.787803	1.194280
						0.4	1.2	-1.20971	-0.66238	0.328135	1.028997
							1.6	-1.20971	-0.66238	0.469168	1.058742
							2	-1.20971	-0.66238	0.651255	1.101407

Table 2: Numerical results of $f''(0), g''(0), Nu/Re_x^{0.5}$ and $Sh/Re_x^{0.5}$ for different values of $Sc, \beta_1, \beta_2, C_1, \delta, n,$ and σ.

Sc	β_1	β_2	C_1	δ	n	σ	$f''(0)$	$g''(0)$	$Nu/Re_x^{0.5}$	$Sh/Re_x^{0.5}$
0.5	0.2	0.2	0.6	1	0.8	5	-1.20971	-0.66238	0.651255	1.101407
0.5							-1.20971	-0.66238	0.651255	1.101407
1							-1.20971	-0.66238	0.651255	1.609301
2							-1.20971	-0.66238	0.651255	2.328783
	0.05						-1.15868	-0.63681	0.683357	1.090295
	0.1						-1.17584	-0.64542	0.672732	1.093920
	0.2						-1.20971	-0.66238	0.651255	1.101407
		0.05					-1.33876	-0.73451	0.596338	1.120828
		0.1					-1.29127	-0.70791	0.616924	1.113429
		0.2					-1.20971	-0.66238	0.651255	1.101407
			0.4				-1.19320	-0.41064	0.579046	1.118408
			0.5				-1.20160	-0.53311	0.617276	1.108962
			0.6				-1.20971	-0.66238	0.651255	1.101407
				1			-1.20971	-0.66238	0.651255	1.101407
				2			-1.20971	-0.66238	0.651255	1.421285
				3			-1.20971	-0.66238	0.651255	1.701805
					0.4		-1.20971	-0.66238	0.521741	1.069771
					0.6		-1.20971	-0.66238	0.604609	1.081346

International Journal of Engineering Research & Technology (IJERT)
ISSN: 2278-0181
Vol. 14 Issue 11, November 2025

					0.8		-1.20971	-0.66238	0.651255	1.101407
						2	-1.20971	-0.66238	0.651255	0.772735
						3	-1.20971	-0.66238	0.651255	0.895297
						5	-1.20971	-0.66238	0.651255	1.101407

References

1. M. Sajid, Z. Abbas, T. Javed and N. Ali, Boundary layer flow of an Oldroyd-B fluid in the region of stagnation point over a stretching sheet, Canadian J. of Phys., **88,** 635-640 (2010).
2. S. A. Shehzad, A.Alsaedi, T. Hayat. and M. S. Alhuthali, Three-dimensional flow of an OldroydB fluid with variable thermal conductivity and heat generation/absorption. PLoS One, **8**, e78240 (2013).
3. T.Hayat,Z.Hussain, M.Farooq, A. Alsaedi and M.Obaid, Thermally stratified stagnation point flow of an Oldroyd-B fluid. International Journal of Nonlinear Sciencesand Numerical Simulation, **15**, 77–86 (2014).
4. S. S. Motsa, Z. G. Makukula,and S. Shateyi, Numerical investigation of the effect of unsteadiness on three-dimensional flow of an Oldroyd-B fluid. PLoS One, **10**, e0133507 (2015).
5. T. Hayat, M. Imtiaz and A. Alsaedi,Boundary layer flow of Oldroyd-B fluid by exponentially stretching sheet, Appl. Math. Mech., **37(5),** 573–582 (2016).
6. B.Mahanthesh, B.J. Gireesha, S.A. Shehzad, F. M. Abbasi and R.S.R. Gorla, Nonlinear three-dimensional stretched flow of an Oldroyd-B fluid with convective condition, thermal radiation,and mixed convection, Appl. Math. Mech. -Engl. Ed., **38(7),** 969-980 (2017).
7. N. Raza, E. U. Haque, M. M. Rashidi, A. U. Awan1 and M. Abdullah, Oscillating motion of an Oldroyd-B fluid with fractionalderivatives in a circular cylinder, Journal ofApplied Fluid Mechanics, **10(5),** 1421-1426 (2017).
8. N. Sandeep and M. Gnaneswara Reddy, MHD Oldroyd-B fluid flow across a melting surface with cross diffusion and double stratification, Eur. Phys. J. Plus, **132**: 147(2017).
9. Tasawar Hayat, Ikram Ullah, Taseer Muhammad, Ahmed Alsaedi, Thermal and solutal stratification in mixed convection three-dimensional flow of an Oldroyd-B nanofluid, Results in Physics **7** 3797–3805 (2017).

International Journal of Engineering Research & Technology (IJERT)
ISSN: 2278-0181
Vol. 14 Issue 11, November 2025

10. Constantin Fetecau, Dumitru Vieru, Corina Fetecau And Itrat Abas Mirza, Effects of fractional order on convective flow of an oldroyd-b fluid along a moving porous hot plate with thermal diffusion, Heat Transfer Research **48(12)**:1047–1068 (2017).

11. O.D. Makinde, Free convection flow with thermal radiation and mass transfer past a moving vertical porous plate, Int. Comm. Heat and mass transfer, **32** 1411-1419 (2005).
12. M.M. Nandeppanavar, K. Vajravelu, M. Subhas, Heat transfer in MHD viscoelastic boundary layer flow over a stretching sheet with thermal radiation and non-uniform heat source/sink, Int. Commun Nonlinear Sci Numer Simulat, **16** 3578-3590 (2011).
13. B.J. Gireesha, B. Mahanthesh, Perturbation solution for radiating viscoelastic fluid flow and heat transfer with convective boundary condition in non-uniform channel with Hall current and chemical reaction, ISRN Thermodynamics **2013**, 935481 14 ,http://dx.doi.org/10.1155/2013/935481 (2013).
14. S.A. Shehzad, F.E. Alsadi, T. Hayat, S.J. Monaquel, MHD mixed convection flow of thixotropic fluid with thermal radiation, Heat Transfer Research, **45** 659-676 (2014).
15. M. M. Rashidi, N. V.Ganesh, A. K. A. Hakeem and B. Ganga, Buoyancy effect on MHD flow of nanofluid over a stretching sheet in the presence of thermal radiation. Journal of Molecular Liquids, **198**, 234–238 (2014).
16. A. Mushtaq, M. Mustafa, T. Hayat, A. Alsaedi, Effects of thermal radiation on the stagnation point flow of upper-convicted Maxwell fluid over a stretching sheet, J. Aerosp. Egg. **27(4)** 10.1061/(ASCE)AS.1943-5525.0000361 (2014).
17. T. Hayat, M. Waqas, S. A. Shehzad, and A. Alsaedi, A model of solar radiation and Joule heating in magnetohydrodynamic (MHD) convective flow of thixotropic nanofluid. Journal of Molecular Liquids, **215**, 704–710 (2016).
18. A. Pantokratoras, T. Fang, Sakiadis flow with nonlinear Rosseland thermal radiation, Science, **26** 161-167 (2014).
19. A. Mushtaq, M. Mustafa, T. Hayat and A. Alsaedi, Nonlinear radiative heat transfer in the flow of nanofluid due to solar energy: a numerical study. Journal of the Taiwan Institute of Chemical Engineers, **45**, 1176–1183 (2014).
20. R. Cortell, Fluid flow and radiative nonlinear heat transfer over a stretching sheet. Journal of King Saud University of Sciences, **26**, 161–167 (2014).

International Journal of Engineering Research & Technology (IJERT)
ISSN: 2278-0181
Vol. 14 Issue 11, November 2025

21. S. A. Shehzad, T. Hayat, A.Alsaedi and M. A. Obid, Nonlinear thermal radiation in threedimensional flow of Jeffrey nanofluid: a model for solar energy. Applied Mathematics and Computation, **248**, 273–286 (2014).
22. T. Hayat, M. Imtiaz, A. Alsaedi and M.A. Kutbi, "MHD three-dimensional flow of nanofluid with velocity slip and nonlinear thermal radiation", J. Magnetism and Magnetic Materials, **396** 31-37 (2015).
23. P.B. Sampath Kumar, B.J. Gireesha, B. Mahanthesh, and R.S.R. Gorla, Radiative nonlinear 3D flow of Ferrofluid with Joule heating, convective condition and Coriolis force, Thermal Science and Engineering Progress, **3** 88–94 (2017).
24. B. Mahanthesh, B.J. Gireesha and R.S.R. Gorla, "Nonlinear radiative heat transfer in MHD three-dimensional flow of water based nanofluid over a non-linearly stretching sheet with convective boundary condition", J. Nigerian Math. Soc., **35** 178-198 (2016).
25. M. Farooq, M.I. Khan, M. Waqas, T. Hayat, A. Alsaedi, M.I. Khan, MHD stagnation point flow of viscoelastic nanofluid with non-linear radiation effects, Journal of Molecular Liquids, 221 1097-1103 (2016).
26. T.V. Laxmi, B. Shankar, Effect of nonlinear thermal radiation on boundary layer flow of viscous fluid over nonlinear stretching sheet with injection/suction, Journal of Applied Mathematics and Physics, **04(02)** 13 – 14 (2016).
27. B.M. Jayachandra, N. Sandeep, C.S.K. Raju, R.J.V. Ramana, V. Sugunamma, Nonlinear thermal radiation and induced magnetic field effects on stagnation-point flow of Ferro fluids, Journal of Advanced Physics, **5(4)** 302-308 (2016).

Published by :
http://www.ijert.org

International Journal of Engineering Research & Technology (IJERT)
ISSN: 2278-0181
Vol. 14 Issue 11, November 2025

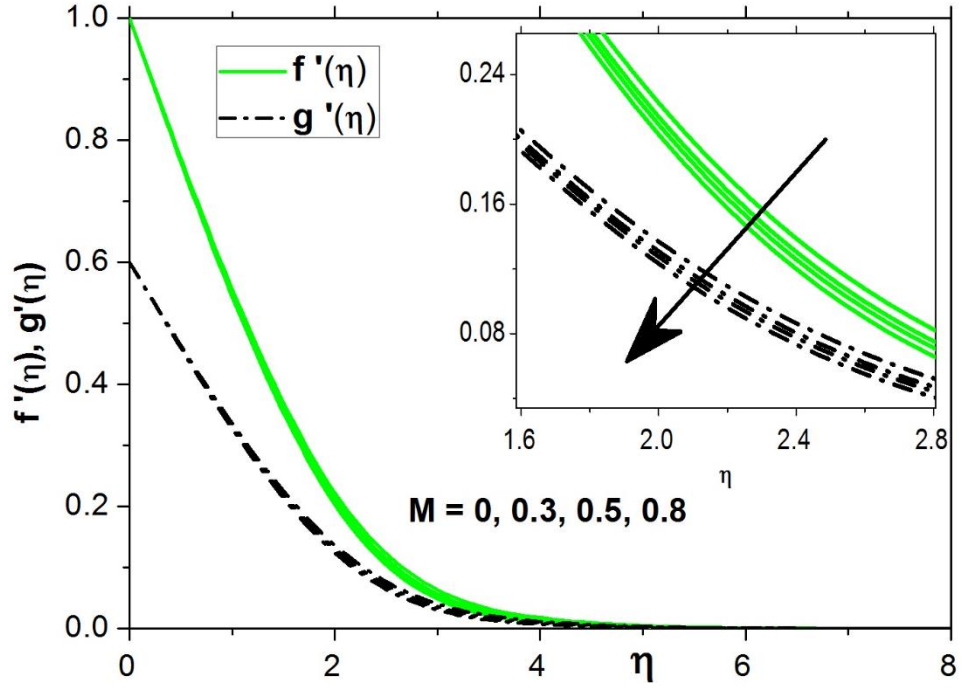

Fig 2: Impact of M on $f'(\eta)$ and $g'(\eta)$.

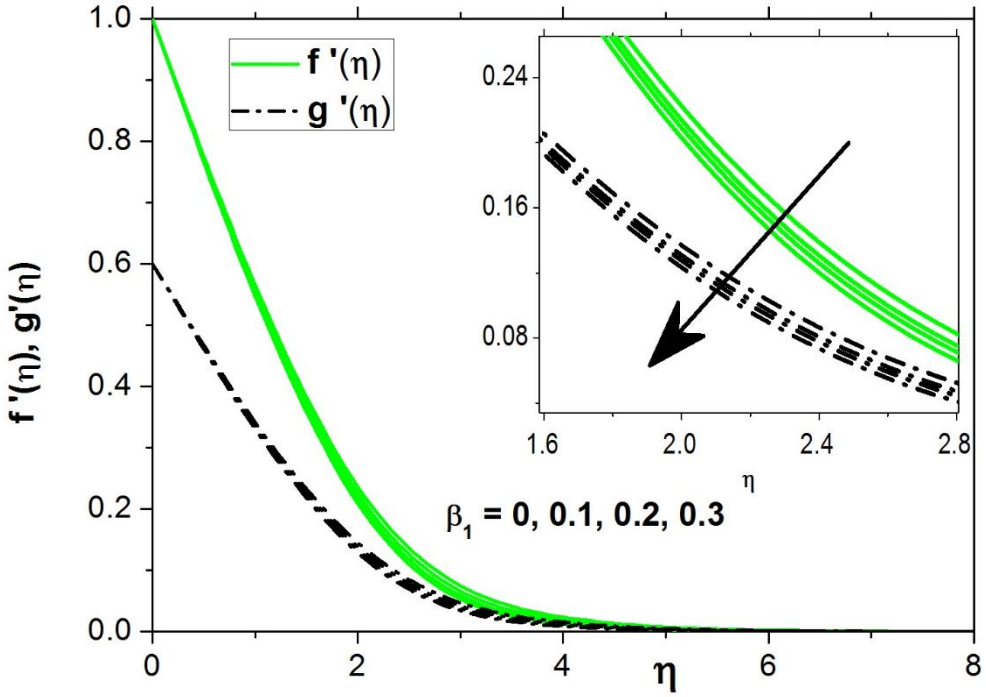

Fig 3: Impact of β_1 on $f'(\eta)$ and $g'(\eta)$.

Published by :
http://www.ijert.org

International Journal of Engineering Research & Technology (IJERT)
ISSN: 2278-0181
Vol. 14 Issue 11, November 2025

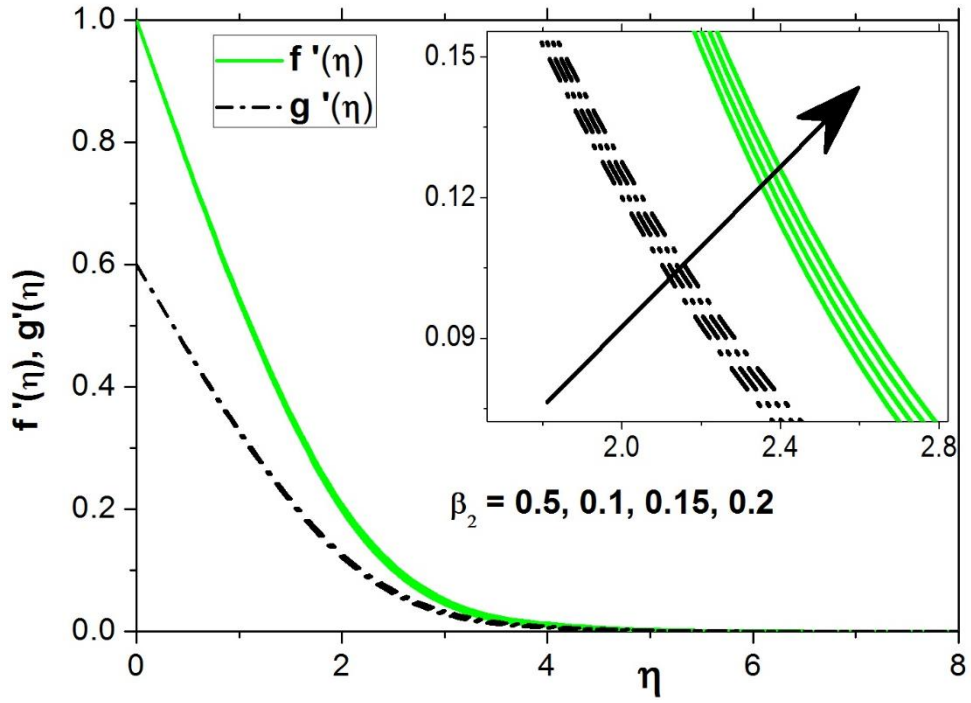

Fig 4: Impact of β_2 on $f'(\eta)$ and $g'(\eta)$.

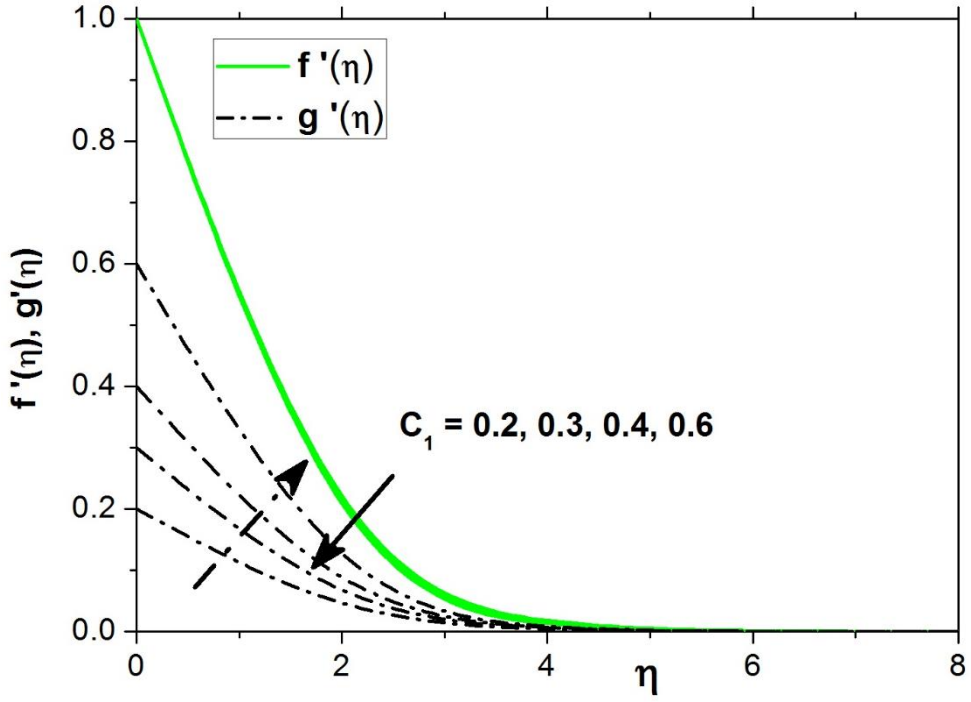

Fig 5: Impact of C_1 on $f'(\eta)$ and $g'(\eta)$.

Published by :
http://www.ijert.org

International Journal of Engineering Research & Technology (IJERT)
ISSN: 2278-0181
Vol. 14 Issue 11, November 2025

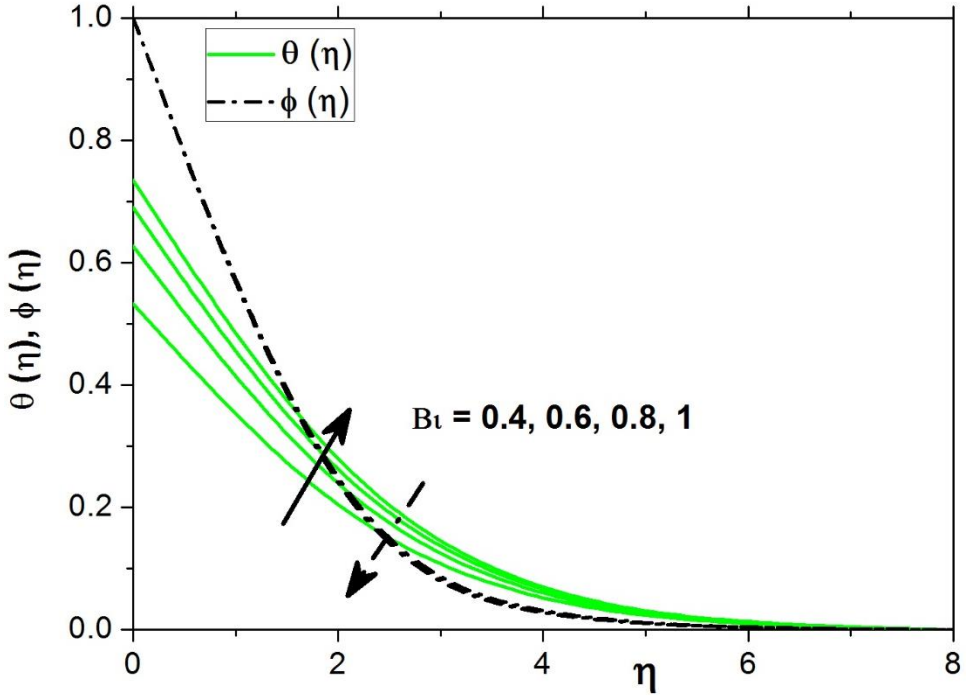

Fig 6: Impact of Bion $\theta(\eta)$ and $\phi(\eta)$.

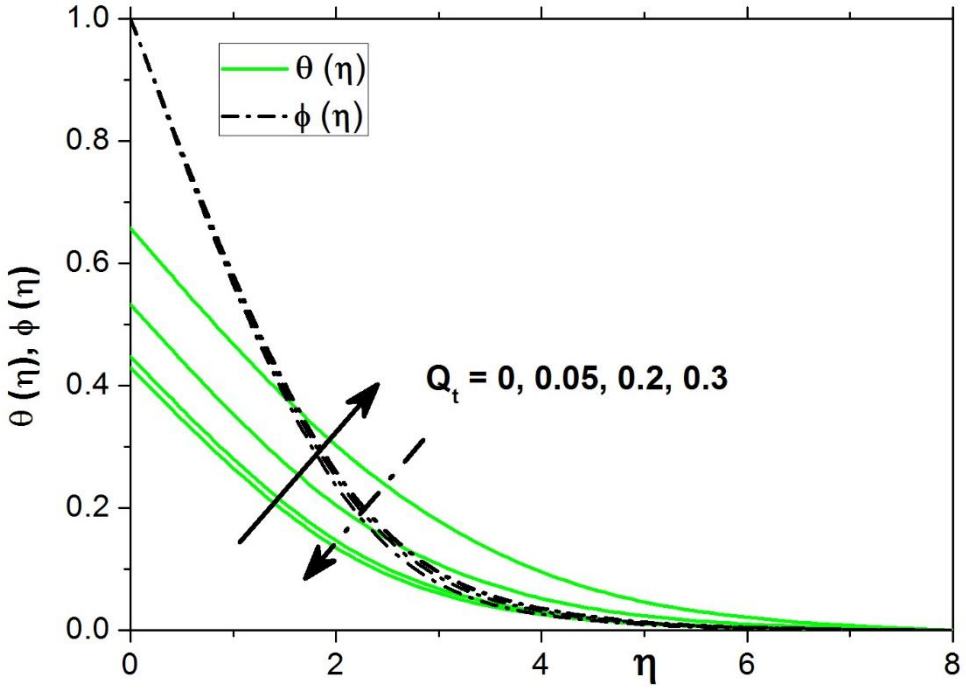

Fig 7: Impact of $Q_t$on $\theta(\eta)$ and $\phi(\eta)$.

International Journal of Engineering Research & Technology (IJERT)
ISSN: 2278-0181
Vol. 14 Issue 11, November 2025

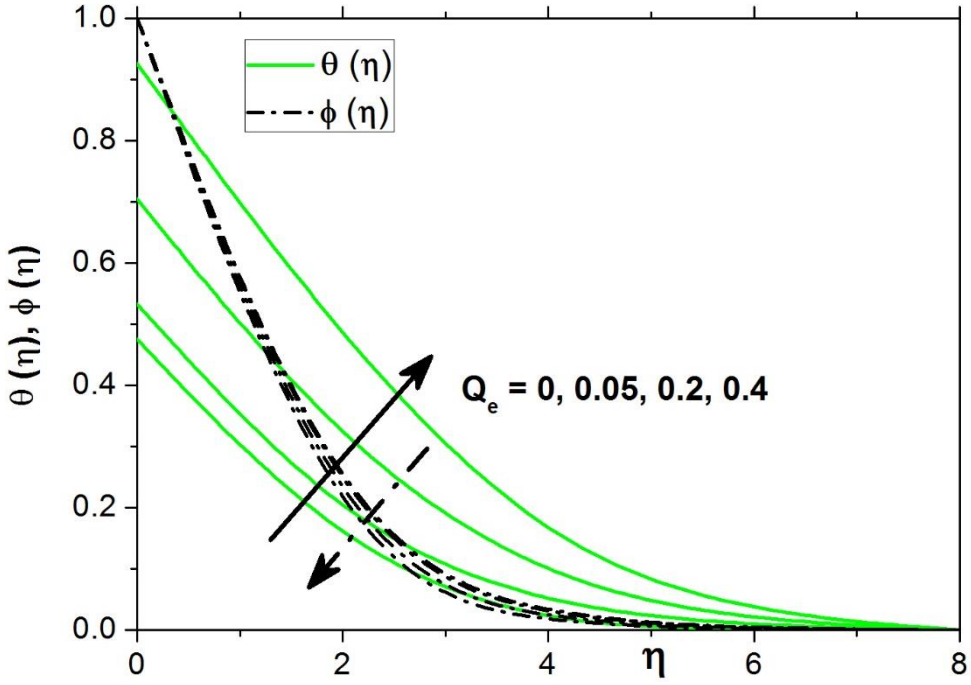

Fig 8: Impact of Q_e on $\theta(\eta)$ and $\phi(\eta)$.

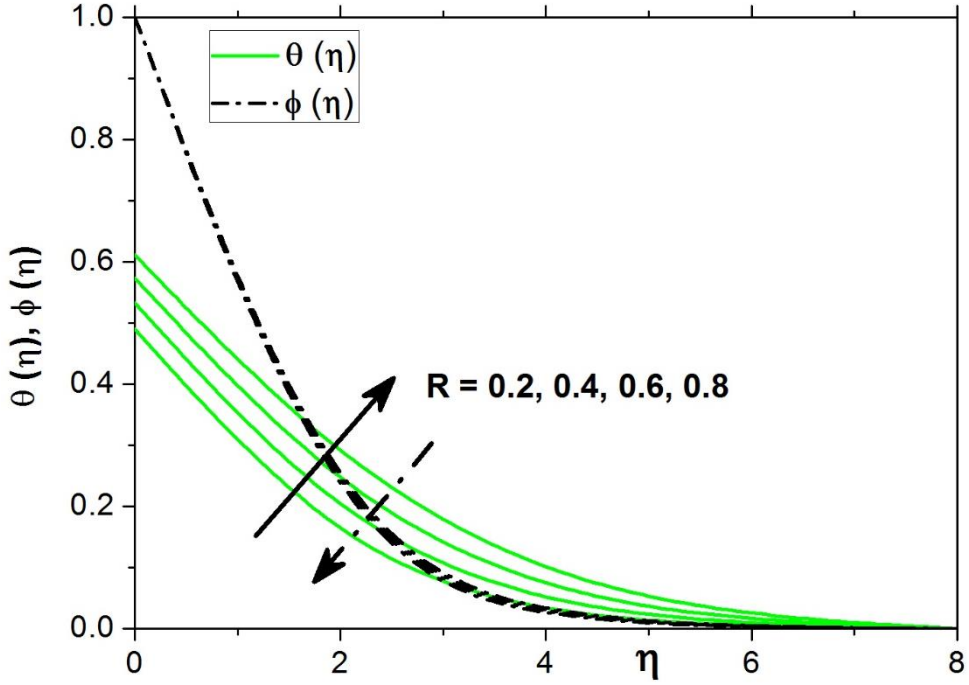

Fig 9: Impact of R on $\theta(\eta)$ and $\phi(\eta)$.

Published by :
http://www.ijert.org

International Journal of Engineering Research & Technology (IJERT)
ISSN: 2278-0181
Vol. 14 Issue 11, November 2025

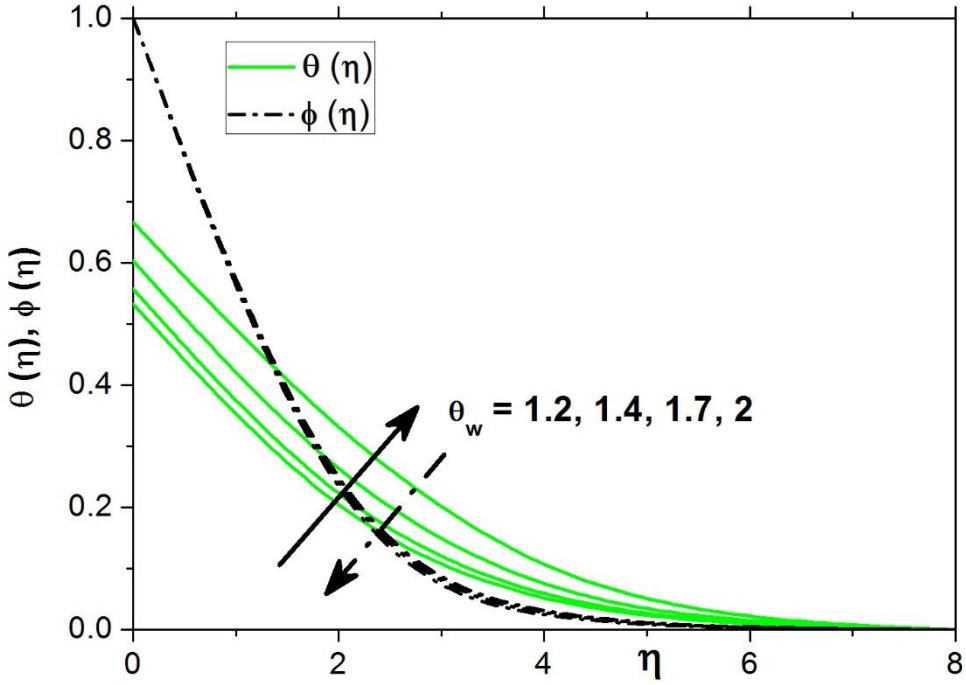

Fig 10: Impact of θ_w on $\theta(\eta)$ and $\phi(\eta)$.

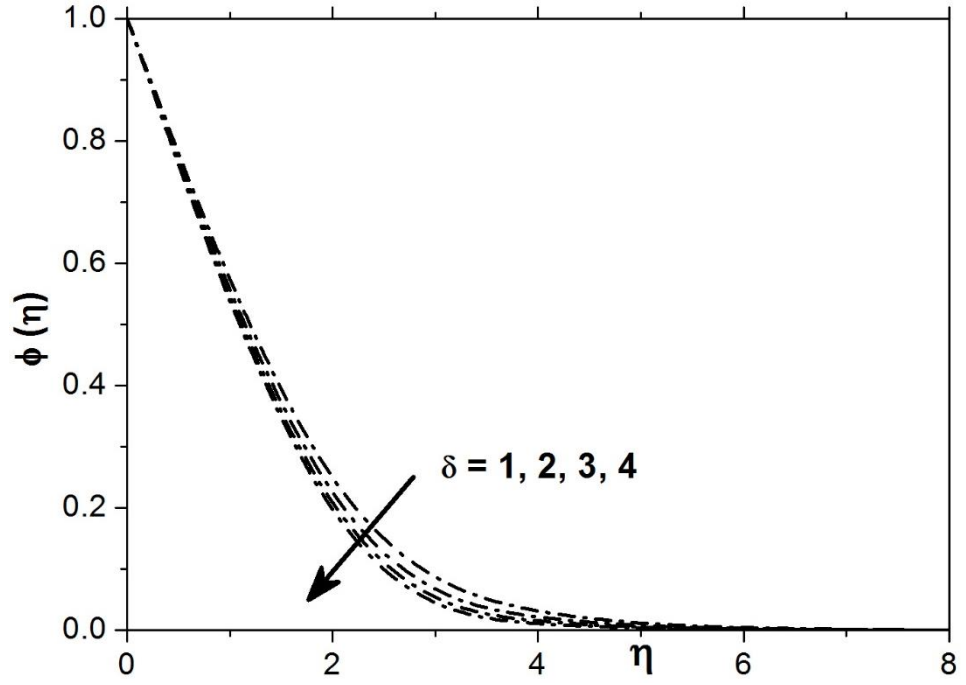

Fig 11: Impact of δ on $\phi(\eta)$.

Published by :
http://www.ijert.org

International Journal of Engineering Research & Technology (IJERT)
ISSN: 2278-0181
Vol. 14 Issue 11, November 2025

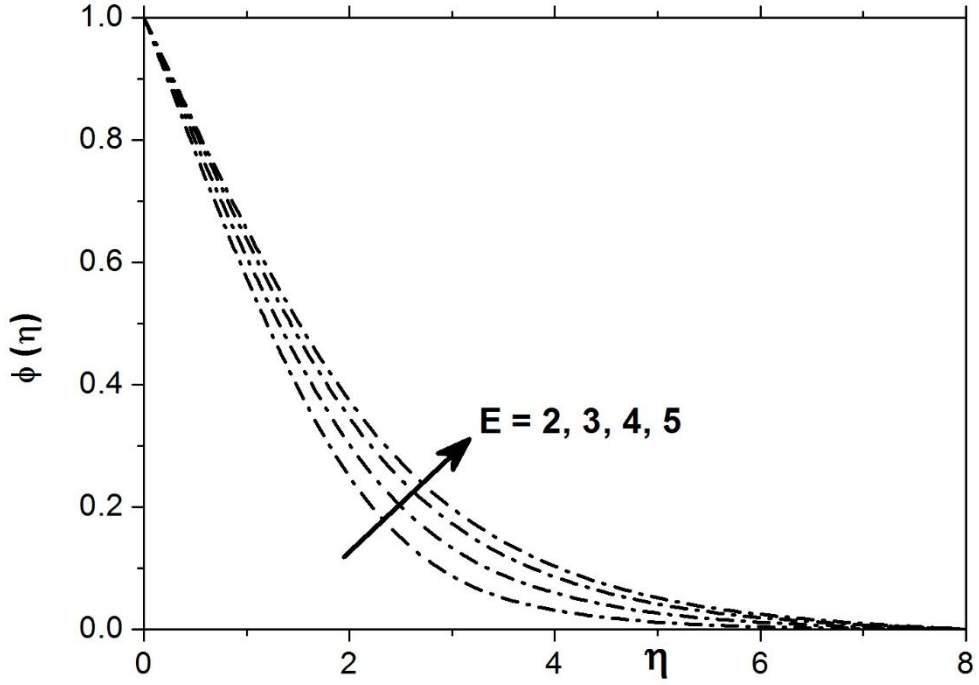

Fig 12: Impact of E on $\phi(\eta)$.

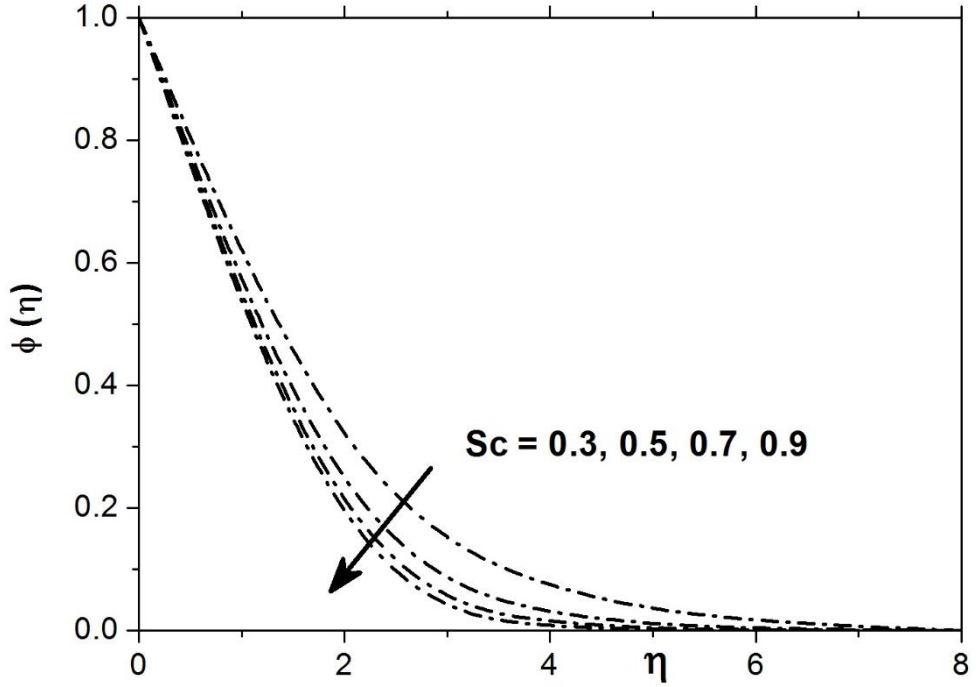

Fig 13: Impact of Sc on $\phi(\eta)$.

International Journal of Engineering Research & Technology (IJERT)
ISSN: 2278-0181
Vol. 14 Issue 11, November 2025

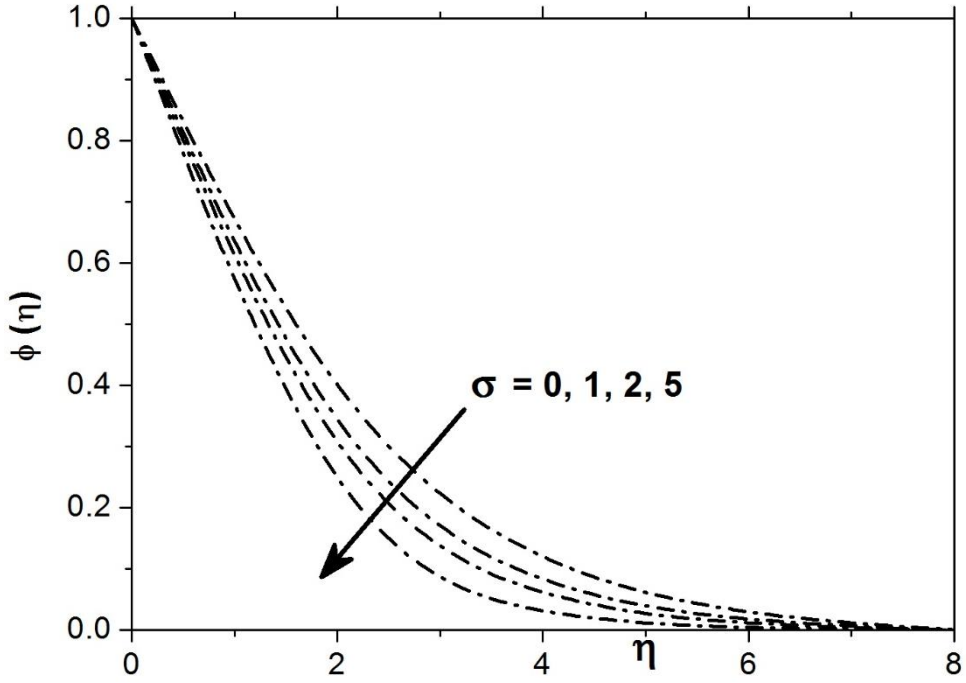

Fig 14: Impact of δon$\phi(\eta)$.